anpet
brazilian association for transportation research and education
TRANSPORTES
ISSN: 2237-1346
anpet.org.br/transportes

Analysis of thermal and hydraulic performance of pervious concrete overlay under clogging conditions

Análise do desempenho térmico e hidráulico de revestimento de concreto permeável em condições de colmatação

Karina de Lima[1], Larissa Virgínia da Silva Ribas[1,2], Antônio Celso Dantas Antonino[3], Antônio Eduardo Bezerra Cabral[1], Verônica Teixeira Franco Castelo Branco[1]

[1]Federal University of Ceará, Fortaleza, Ceará, Brasil
[2]Federal University of Bahia, Salvador, Bahia, Brasil
[3]Federal University of Pernambuco, Recife, Pernambuco, Brasil

Contact: karina.lima@det.ufc.br, (KL); larissa.ribas@det.ufc.br, (LVSR); acdantonino@gmail.com, (ACDA); eduardo.cabral@ufc.br, (AEBC); veronica@det.ufc.br (VTFCB)

Submitted:
25 April, 2025
Revised:
15 August, 2025
Accepted for publication:
7 September, 2025
Published:
19 January, 2026
Associate Editor:
Francisco Thiago Sacramento Aragão, Universidade Federal do Rio de Janeiro, Brasil

Keywords:
Urban heat island mitigation.
Permeable pavements.
Thermal performance.
Pore clogging.
Hydraulic performance.

Palavras-chave:
Mitigação de ilhas de calor urbanas.
Pavimentos permeáveis.
Desempenho térmico.
Colmatação de poros.
Desempenho hidráulico.

DOI: 10.58922/transportes.v33.e3119

ABSTRACT
Accelerated urban growth results in soil impermeabilization, intensifying problems such as floods and urban heat islands (UHIs) formation. Pervious concrete pavement (PCP) is a strategy used to mitigate these problems, with the capacity to regulate stormwater runoff and its low thermal conductivity. However, clogging, caused by the infiltration of sediments, obstructs the pores of the PCP, compromising its hydraulic and thermal performance. This study investigates the effects of clogging on PCP overlay, with a focus on thermal behavior and conductivity. Initially, air temperature and humidity were evaluated to understand their influence on the surface temperatures of the clean PCP. When comparing the unclogged and clogged PCPs, the unclogged PCP showed surface temperatures on average 1.25 °C higher than the clogged ones under solar exposure. The thermal conductivity analysis revealed the impact of clogging with sand, which has a conductivity 85.7% higher than air. The results indicate that, although clogging impairs hydraulic performance, it improves thermal performance. These findings suggest that the balance between hydraulic and thermal behaviors must be evaluated when managing low-impact development structures.

RESUMO
O crescimento urbano acelerado resulta na impermeabilização do solo, intensificando problemas como inundações e formação de Ilhas de Calor Urbanas (ICUs). O Pavimento de Concreto Permeável (PCP) é uma estratégia utilizada para mitigar esses problemas, com capacidade de regular o escoamento pluvial e sua condutividade térmica reduzida. No entanto, o entupimento, causado pela infiltração de sedimentos, obstrui os poros do PCP, comprometendo seu desempenho hidráulico e térmico. Este estudo investiga os efeitos do entupimento no PCP, com foco no comportamento térmico e na condutividade do mesmo. Inicialmente, temperatura e umidade do ar foram avaliadas para compreender a influência nas temperaturas superficiais do PCP desobstruído. Ao comparar o PCP desobstruído e o obstruído, o PCP desobstruído apresentou temperaturas superficiais em média 1,25 °C mais altas do que os obstruídos sob exposição solar. A análise da condutividade térmica revelou o impacto do entupimento com areia, que possui condutividade 85,7% maior que o ar. Os resultados indicam que, embora o entupimento prejudique o desempenho hidráulico, ele melhora o desempenho térmico. Essas descobertas sugerem que o equilíbrio entre os comportamentos hidráulico e térmico deve ser avaliado ao gerenciar estruturas de desenvolvimento de baixo impacto.

1. INTRODUCTION

The expansion of urban areas, driven by demographic increases, rapid urbanization, and infrastructure development, has progressively replaced vegetated surfaces with low-permeability pavements (Seifeddine, Amziane and Toussaint, 2023; Wang et al., 2018). This transformation has resulted in inefficient drainage and intensified heat dissipation, exacerbating disruptions in the hydrological cycle and worsening urban thermal discomfort (Guan, Wang and Xiao, 2021). These conditions contribute to the formation of Urban Heat Islands (UHI), a phenomenon characterized by elevated temperatures in urbanized areas compared to their surrounding regions (Taleghani, 2018). The porous structure of pervious concrete facilitates groundwater recharge, reduces noise generated by tire-pavement interaction and decreases runoff velocity (Wang et al., 2022; Xie, Akin and Shi, 2019).

The increased velocity of stormwater runoff can lead to erosion, channel widening, sediment deposition, flooding, and pollutant dispersion in downstream areas, effects linked to reduced soil permeability and its negative environmental implications (Kovác and Sicáková, 2017). Unregulated urbanization is a significant driving force influencing surface runoff dynamics (Chen et al., 2019a).

Adopting permeable pavements offers an effective alternative for optimizing drainage systems and managing stormwater runoff, thereby contributing to reduced infrastructure costs (Moretti, Di Mascio and Fusco, 2019). Moreover, the cooling effect enabled by evaporation, due to water retention within the pavement's pores, enhances thermal dissipation following rainfall events (Bonicelli and Pianeta, 2019). Additionally, these pavements exhibit lower thermal conductivity compared to standard materials. Studies indicate that interlocking concrete pavements present thermal conductivity values between 1.33 and 1.95 W/m·K (Hendel et al., 2018; Bin Yahaya, 2010), asphalt pavements range from 1.55 to 2.06 W/m·K (Hendel et al., 2018) and Portland cement concrete falls between 1.14 and 2.01 W/m·K (Hendel et al., 2018). In contrast, pervious concrete exhibits an average thermal conductivity approximately 60% lower than that of asphalt pavements, ranging from 0.43 to 0.82 W/m·K (Chen et al., 2019b; Nassiri and Nantasai, 2017), which is primarily attributed to the air entrapped within its porous structure. This lower thermal conductivity makes pervious concrete highly efficient in reducing surface temperatures and mitigating UHI effects.

Kia, Wong and Cheeseman (2017) highlight that there is a wide variation in the mass proportions used in pervious concrete mix designs. These variations range from a ratio of 1:0.73:0.2 (cement: coarse aggregate: water/cement (ratio)) to 1:0.14:4.00:0.50 (cement: fine aggregate: coarse aggregate: ratio). Pervious concrete contains interconnected pores, which account for a significant percentage (between 15% and 35%) of its total structure (El-Hassan, Kianmehr and Zouaoui, 2019; Seifeddine, Amziane and Toussaint, 2022). These pores play a crucial role in heat exchange between the concrete and the environment, influencing its thermal conductivity and capacity to mitigate temperature variations.

It is important to note that, as emphasized by Yang et al. (2020), the surface temperature of PCP is affected by the surrounding environmental conditions. Moreover, the thermal performance of pervious concrete is associated with the evaporation process. Under humid conditions, infiltrated water evaporates slowly, utilizing part of the heat stored on the pavement surface, which results in a lower temperature increase compared to dense concrete pavements (Rossetto et al., 2023). However, the efficiency of this process depends on the moisture level within the material. On dry days, pervious concrete can reach surface temperatures up to 5°C higher due to the absence of continuous evaporation (Chen et al., 2019a).

The permeability of PCP can be compromised due to pore clogging, a process characterized by the gradual obstruction of void spaces caused by the infiltration of sediments and organic

particles. This leads to a reduction in permeability and degradation of the performance of PCP (Yuan et al., 2018). The significance of the clogging level in pervious concrete, concerning surface temperature variation, lies in its impact on water absorption, which is inversely related to the rate of temperature increase in the pavement (Wang et al., 2018). The evaporation process, on the pavement surface, utilizes a portion of the absorbed heat to convert water into vapor, thereby mitigating surface heating (Chen et al., 2019a).

Clogging can interfere with this evaporative cooling process in PCP, playing a role in minimizing the effects of UHI (Wang et al., 2018). As highlighted by Chen et al. (2019b), the thermal conductivity of pervious concrete tends to decrease as porosity increases, indicating that pore-clogging negatively affects the thermal conductivity of these pavements, as it favors their heating by increasing their thermal conductivity. Therefore, this study aims to investigate the thermal behavior of PCP by comparing the performance of clean and clogged surfaces, to optimize the use of this material in mitigating UHI.

2. EXPERIMENTAL

The methodology employed in this study was structured into three main stages:

1) Molding and characterization of Pervious Concrete Pavement (PCP) boards;

2) Characterization of the clogging material and the clogging process;

3) Thermal tests.

The experimental program is summarized in Figure 1, which visually illustrates the steps and tools utilized in each phase of the study.

2.1. Molding and characterization of the PCP blocks

The PCP blocks were produced using a TPrex VibroPress machine, with a concrete mix proportion of 1:0.74:2.48:0.33 (cement: sand: gravel: w/c). The blocks, measuring 40 × 40 × 8 cm, were classified according to ASTM C1701/C1701M for light traffic (ASTM, 2023). Portland cement CPV ARI was chosen as the binder due to its high early-age compressive strength, which facilitated rapid demolding (Isaia, 2007). The fine aggregate was a quartz river sand with a maximum particle size of 4.8 mm, and the coarse aggregate used was granite with a maximum nominal size of 9.5 mm. The gradation curves of these materials are presented in Figure 2.

The pervious concrete blocks were characterized following the procedures of ASTM C642 (ASTM, 2021c), analyzing water absorption, void ratio, and specific gravity. The masses in dry, saturated, and submerged conditions were determined using hydrostatic and standard scales, enabling the calculation of these parameters. The permeability test for the PCP blocks was conducted based on an adapted method from ASTM C1701/C1701M (ASTM, 2023). To evaluate flexural strength, the blocks were characterized following the test recommendations of ASTM C78/C78M (ASTM, 2022).

Due to space limitations in the drying oven used in the study, the blocks were reduced to dimensions of 20 × 20 × 8 cm, maintaining the original thickness of 8 cm. To achieve this, the blocks were initially cast in their full dimensions (40 × 40 × 8 cm) and subsequently cut using a water-cooled diamond blade saw. This procedure was adopted to ensure compatibility with the equipment while preserving the technical feasibility of the experimental program. Although cutting hardened blocks may affect edge uniformity or induce microcracks, the process was conducted with technical rigor to minimize such effects, following recommendations from the

literature (Mindess, 2019; Neville, 1995). Moreover, prior studies indicate that when the cut surfaces are not directly loaded and quality control is applied, no significant impact on the test results is expected. Accordingly, the adopted procedure proved technically adequate under the laboratory constraints. Consequently, the ring size and water volume were adjusted for the test, considering the reduced contact area. A ring with a diameter of 200 mm was used, and the water volume was adjusted to 8 liters.

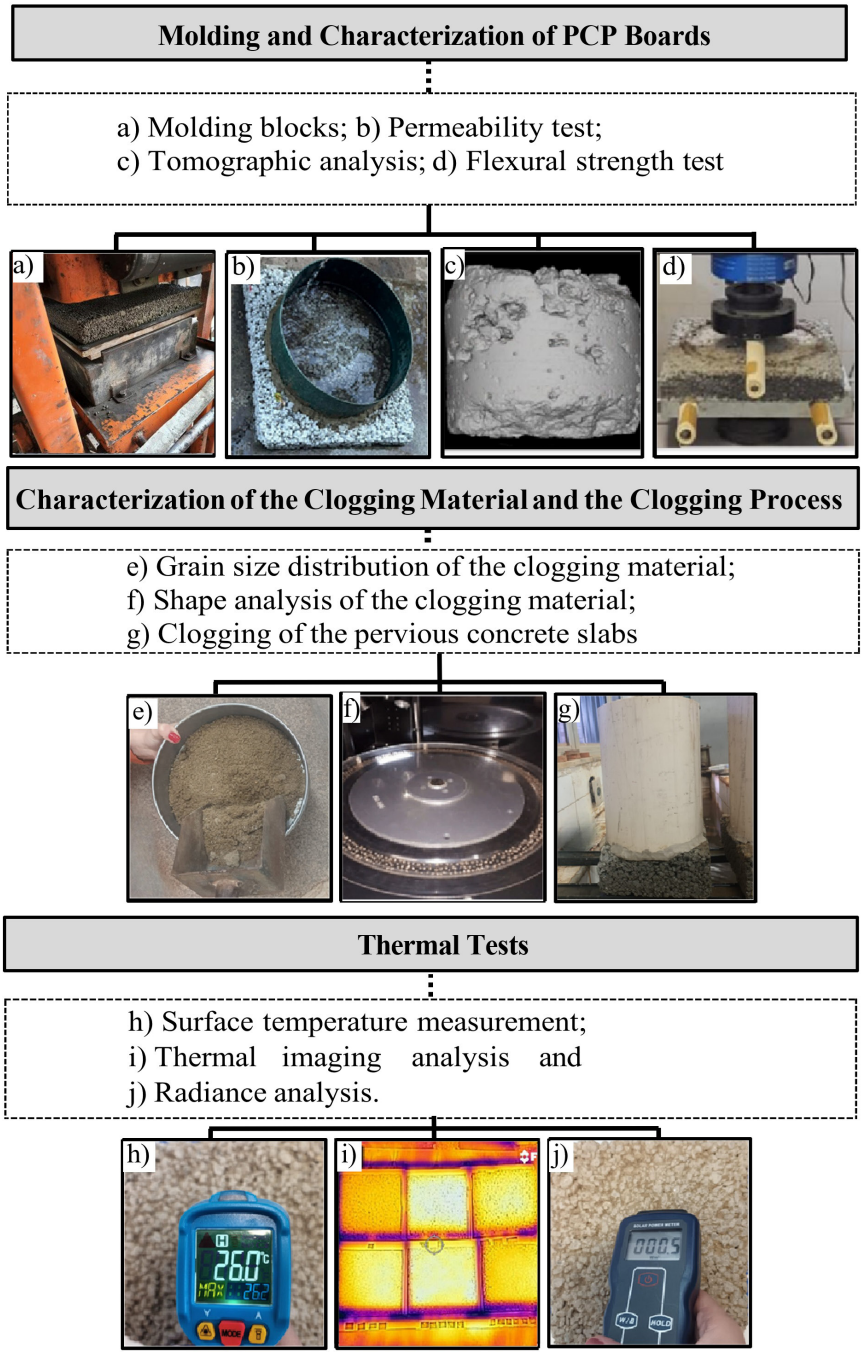

Figure 1. Methodology used for the thermal characterization of clean and clogged pervious concrete blocks (a) Molding PCP blocks; (b) Permeability test of PCP blocks; (c) Tomographic analysis of PCP blocks; (d) Flexural strength test of PCP blocks; (e) Grain size distribution of the clogging material for PCP blocks; (f) Shape analysis of the clogging material for PCP blocks; (g) Clogging of the PCP blocks; (h) Surface temperature measurement of PCP blocks; (i) Thermal imaging analysis of PCP blocks; (j) Radiance analysis of PCP blocks.

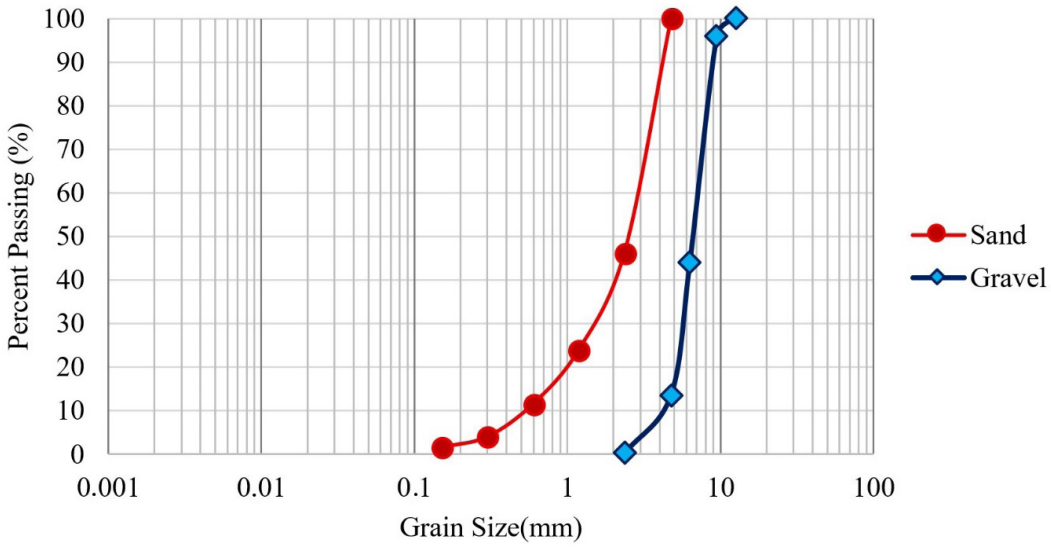

Figure 2. Gradation curves of the materials (sand and gravel) used in the PCP blocks.

2.2. Characterization of the clogging material and the clogging process of pervious concrete blocks

The sand used for the clogging process was characterized according to the procedures established by ASTM D6913-04 (ASTM, 2021a), complemented by image analysis based on DNIT 432/2020 standards using the aggregate image measurement system (AIMS) (DNIT, 2020). The clogging of the pervious concrete blocks' voids was performed using sand as the filling material. The sand used in this study for the clogging process was obtained from a riverbed, and its gradation was analyzed. Figure 3 presents the clogging materials gradation.

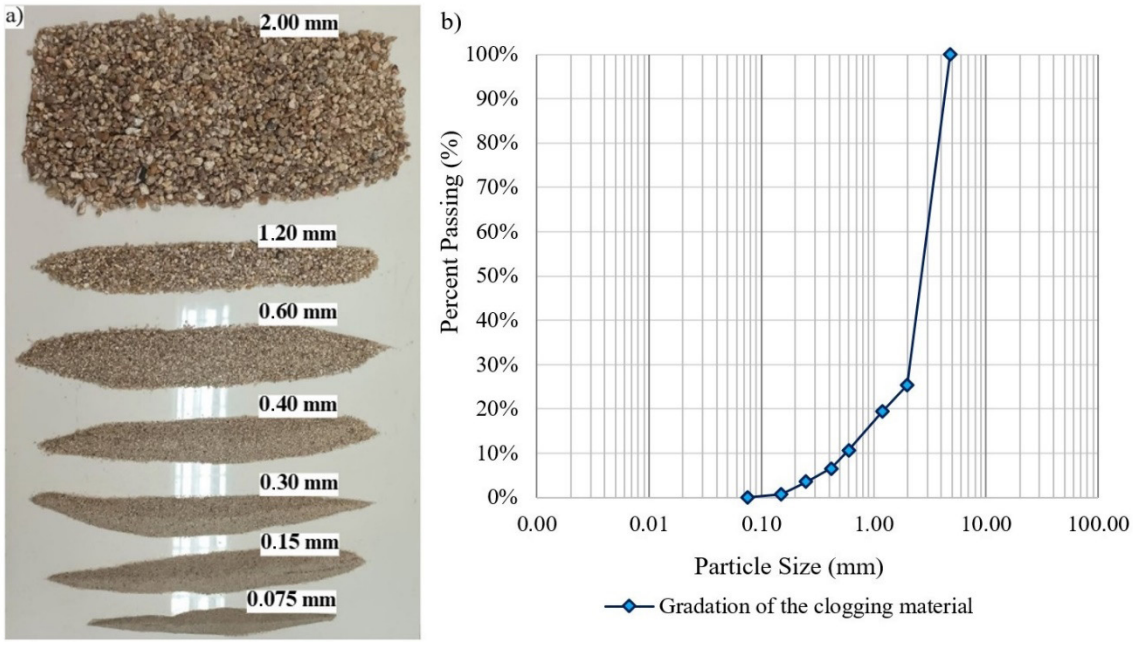

Figure 3. Characterization of the clogging material: (a) Visual representation of the clogging material sorted by sieve size; (b) Gradation of the clogging material.

The clogging process was conducted over 20 cycles, with each cycle involving 3.28 kg of sand and 15.20 liters of water. Two cycles were performed daily with a 10-hour interval between them. The amount of clogging material was based on methods described by Mata (2008) and Tong (2011).

Particles with semicircular angularity, compared to angular ones, are less detrimental to permeability reduction because the lower irregularity of the particles allows for the maintenance of flow channels between the pores (Maroof, Mahboubi and Noorzad, 2020). Furthermore, the semicircular angularity facilitates water accumulation in small voids through surface tension at the air-water interface, making it more favorable for water retention compared to angularity, which tends to hinder this process due to greater flow dispersion (Tahmasebi, 2018).

However, the finer fraction (0.075 mm), with a higher proportion of angular particles (16.39%), may negatively impact hydraulic performance by reducing the permeability of pervious concrete, forming a compact layer that densely fills the pores and hinders water infiltration. This occurs due to the formation of compact layers that densely fill the pores, hindering water infiltration (Maroof, Mahboubi and Noorzad, 2020; Xiong et al., 2023). The angularity and shape distribution of particles were analyzed using the AIMS. This system provides quantitative metrics for particle angularity and texture, which are critical for understanding their impact on permeability and retention properties (Ding et al., 2020). The 2D shape distribution metric, as shown in Figure 4, categorizes particles based on their angularity, ranging from low to extreme.

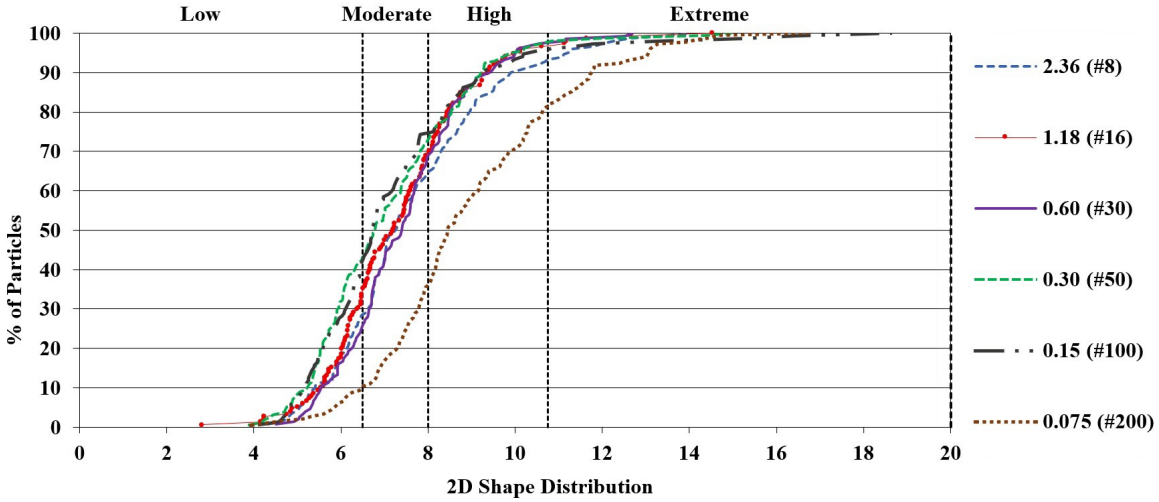

Figure 4. 2D Shape Parameter (AIMS) distribution.

The analysis of the 2D shape distribution of the clogging aggregates, obtained through the AIMS system, revealed that most of the particles exhibit values between 3,000 and 7,000, corresponding to moderate to high angularity, as shown in Figure 5. Smaller particles, such as those in the 0.075 mm (200) fraction, were predominantly concentrated in the low angularity range, with 90% of them below 4,000 in the angularity index. In contrast, larger particles, such as those in the 2.36 mm (#8) fraction, showed greater dispersion, with 50% of the particles reaching values above 5,000, indicating high irregularity. This variation in angularity suggests that larger particles contribute to mechanical interlocking, while smaller, less angular particles, may increase the risk of clogging by easily settling into the pores (Miao et al., 2019). This combination directly affects hydraulic behavior (Xiong, Baychev and Jivkov, 2016).

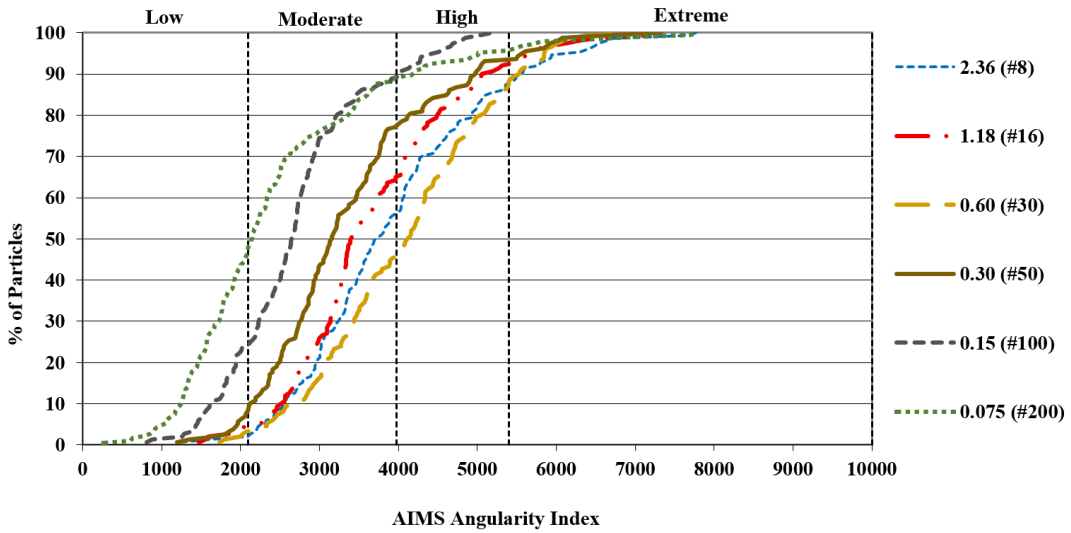

Figure 5. Angularity Index (AIMS) for the clogging material.

2.3. Thermal tests carried at pervious concrete blocks before and after the clogging process

The surface temperature (Ts) of the PCP exposed to the environment (from 5:00 a.m. to 7:00 p.m.) was measured using an MT-350A infrared thermometer and a FLIR C2 thermal camera, at 30-minute intervals. Three HOBO UX100-011A thermohygrometers were positioned at a vertical distance of 2 meters from the ground and a horizontal distance of approximately 15 meters from the tested pervious concrete blocks.

Additionally, the reflected radiance of the pervious concrete blocks in both clean and clogged states was measured using the Solar Power Meter SM206 Digital Solar Power Meter Sun Light Radiation Measuring Testing Instrument for Solar Radiation Measurement. The measurements were taken at a constant distance of 10 cm from the surface of both clean and clogged blocks, ensuring consistency in data collection.

The temperature measurement of the pervious concrete blocks began at 5:30 a.m. and continued until 7:00 p.m., following data provided by the Department of Urban Planning and Environment of Fortaleza, which supplied air temperature and relative humidity data collected from November 2022 to October 2023. As illustrated in Figure 6, the graph depicts the thermal behavior of Fortaleza's air temperature as the average of temperatures recorded during this period. It shows a gradual increase, peaking at 1:00 p.m., followed by a 3 °C drop and a 19% increase in relative humidity by the late afternoon.

In the first stage of the experiment, six pervious concrete blocks in their initial (clean) state, i.e., without clogging, were tested. This phase served as a reference for the subsequent measurements, providing baseline data for comparing the results obtained. The blocks were exposed to direct solar radiation while being thermally insulated from the support substrate to prevent heat transfer through conduction. While this approach was necessary to isolate and analyze the thermal response of the block's surface itself, it does not fully reproduce real-world boundary conditions, where heat transfer to and from the underlying pavement structure plays a significant role. Consequently, the results should be interpreted with this limitation in mind, particularly when extrapolating cooling efficiency and durability to in-field applications.

In the following stage, the same blocks were used, but three of them underwent the clogging process. The experimental procedure followed the same criteria as the previous stage, enabling the analysis of surface temperature variations between the unclogged and clogged states. During the tests, the blocks remained exposed to the sunlight and thermally insulated, as illustrated in Figure 7.

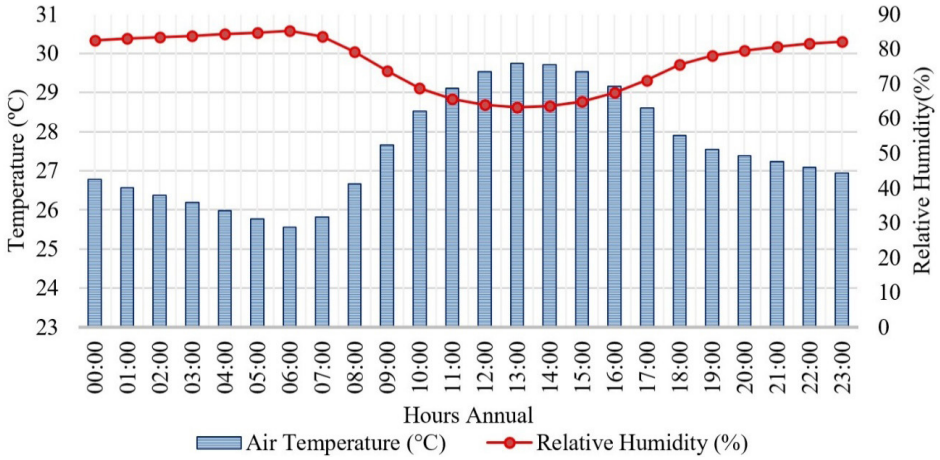

Figure 6. Hourly average air temperature and relative humidity throughout 24 hours.

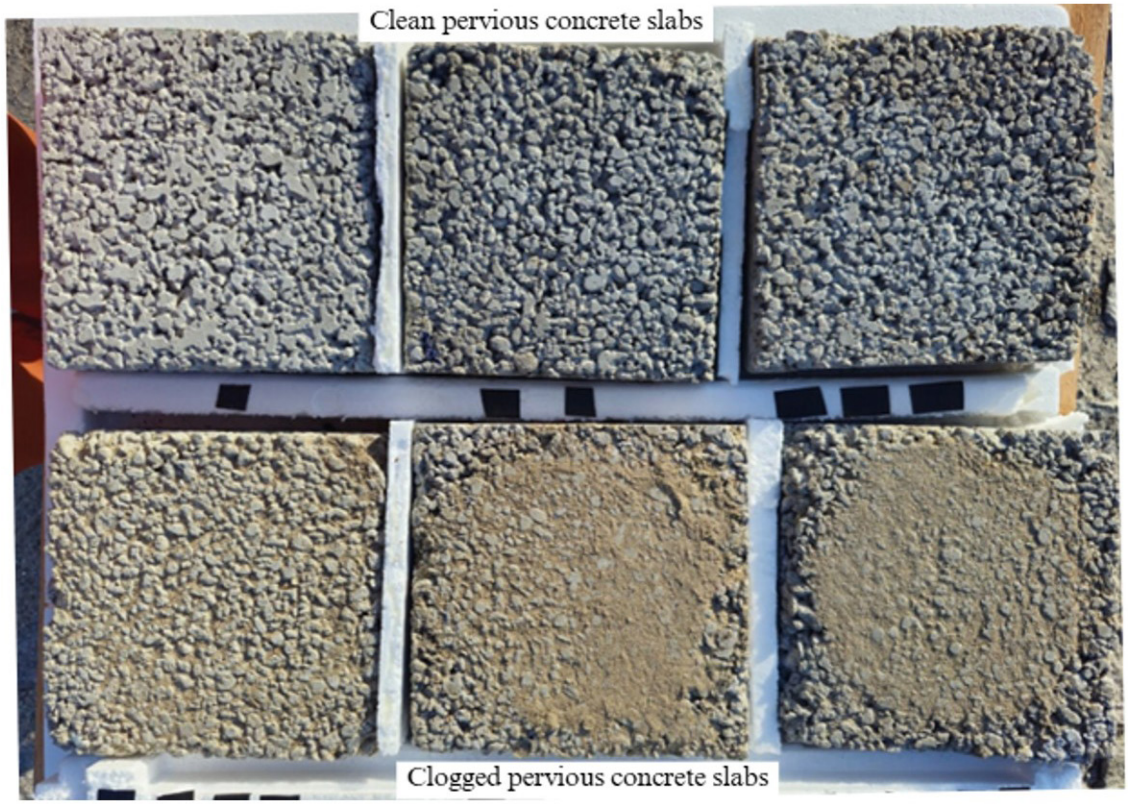

Figure 7. Surface temperature testing configuration for clean and clogged pervious concrete blocks.

Computed tomography was performed using a Nikon Metrology XT H 225 ST tomograph with a resolution of 50 µm and an angular speed of 0.17°/s to analyze the relationship between the concrete volume and void volume in pervious concrete blocks, the images were acquired with software Inspect-X (XT 6.10), reconstructed with CT Pro 3D (XT 6.10), and processed to obtain the parameters using VGSTUDIO MAX (3.4.4). This technique was selected for its ability to generate detailed three-dimensional images of internal microstructures, allowing for non-destructive analysis of porosity and the distribution/size of voids throughout the samples (Merten et al., 2022; Wang et al., 2022).

The analysis focused on segmenting the images to identify and quantify pores along the depth of the samples, utilizing gray threshold segmentation to distinguish filled pores from voids (Lu et al., 2023). Based on the data obtained, a regression model was developed to correlate pore and concrete volumes, aiming to understand the influence of porosity on the material's permeability and thermal properties (Chen et al., 2019b; Tan et al., 2021).

The analysis of thermal conductivity was performed using the method developed by Nassiri and Nantasai (2017), which employs Equation 1 to determine the thermal conductivity of the material. This equation considers the thermal conductivity coefficients of the materials comprising the PCP and its respective proportions in the composition (Zimmerman, 1989).

$$K_{PCP} = \sum_{i=0}^{N} n_i \times K_i \quad (1)$$

where, K_{PCP}: thermal conductivity of the PCP ($W.m^{-1}.k^{-1}$); n_i: proportion of material, N: the composition of the pervious concrete; K_i: thermal conductivity of the material ($W.m^{-1}.k^{-1}$). The proportion of each material in the PCP was determined based on the concrete mix design and on the void index, using Equations 2, 3 and 4, as proposed by Nassiri and Nantasai (2017).

$$n_{ag} = \frac{M_{agG}}{M} \quad (2)$$

$$n_{ag} = \frac{M_{agF}}{M} \quad (3)$$

$$n_p = 1 - \varphi_i - n_{ag} \quad (4)$$

where, n_{ag}: proportion of aggregate in the pervious concrete; M_{agG}: mass of the coarse aggregate (gravel) in 1 m^3 of concrete (kg); M_{agF}: mass of the fine aggregate (sand) in 1 m^3 of concrete (kg); ;M: the total mass of the mix in 1 m^3 of concrete (kg); n_p: proportion of cement paste in the pervious concrete; φ_i : void index of the pervious concrete in its clean state.

Table 1 presents the material proportions for the composition of the PCP in its clean state. The thermal conductivity coefficients used in the analysis were obtained from the literature (Hendel et al., 2018; Nassiri and Nantasai, 2017) and are displayed in Table 2.

Table 1: Material proportions in the composition of six pervious concrete blocks

φ_i	n_{agG}	n_{agF}	n_p
0.15	54.60%	16.20%	14.20%

Table 2: Thermal Conductivity (W.m-1.k-1) of Pervious Concrete Components

Material	Thermal Conductivity ($W.m^{-1}.k^{-1}$)	References
CP V ARI Cement Paste	0.980	Nassiri and Nantasai (2017)
Granite crushed stone	2.160	Hendel et al. (2018)
Air voids	0.026	Nassiri and Nantasai (2017)
Sand	0.183	Nassiri and Nantasai (2017)

To determine the thermal conductivity of the clogged blocks, it was necessary to place them in an oven for 72 hours, allowing their dry weight to be obtained after the clogging process. This was compared with the initial dry weight, without any type of clogging, to obtain the weight of the clogging material in the PCP.

To determine the thermal conductivity of the clogged pervious concrete, it was necessary to calculate the bulk density of the clogging sand, following the guidelines of ASTM D7263-09 (ASTM, 2021b). Equation 5, which is used to calculate the bulk density, is presented below.

$$\rho_{ap} = \frac{m_{ar} - m_r}{V} \tag{5}$$

where, ρ_{ap}: unit weight of the material (kg/m^3); m_{ar}: mass of the material and container together (kg); m_r: mass of the empty container (kg); V: volume of the container (m^3).

Using the bulk density, it was possible to determine the volume of sand used in the clogging. The clogging partially fills the voids in the porous pavement, according to Kia, Wong and Cheeseman (2017). In this context, Equation 6 is used to determine the percentage of this material comparative to the initial volume of voids in the pervious concrete. This approach aims to obtain information about the thermal conductivity of the blocks after the clogging process:

$$n_{clogging} = \frac{V_{clogging}}{Vv} \tag{6}$$

where, $n_{clogging}$: proportion of clogging material occupying the voids in the pervious concrete; $V_{clogging}$: volume the clogging material; V_v: initial volume of void of the pervious concrete.

After determining the proportion of clogging material, this percentage was subtracted from the initial void index using Equation 7, as the clogging material occupies the void spaces in the pervious concrete, as highlighted by Kia, Wong and Cheeseman (2017).

$$\varphi_{after\ clogging} = \varphi_{initial} - n_{clogging} \tag{7}$$

where, $\varphi_{after\ clogging}$: void index of the pervious concrete after clogging; $\varphi_{initial}$: initial void index of the pervious concrete in its clean state; $n_{clogging}$: proportion of clogging material occupying the voids in the pervious concrete.

3. RESULTS AND DISCUSSION

3.1. Characterization of PCP blocks

The characterization of the PCP followed the method established by ASTM C642 (ASTM, 2021c). Figure 8 presents results for water absorption, void ratio and specific gravity for the analyzed blocks. The average water absorption was 5.93%, with a coefficient of variation of 1.11%.

The average void ratio of the blocks was 15.26%, with a coefficient of variation of 0.87%, that is between 15.00% and 35.00% values commonly reported for pervious concretes, ensuring adequate water infiltration capacity (Kia, Wong and Cheeseman, 2017; Merten et al., 2022).The average void ratio of the blocks was 15.26%, with a coefficient of variation of 0.87%, that is between 15% and 35% values commonly reported for pervious concretes, ensuring adequate water infiltration

capacity (Spoorthy and Chandrappa, 2023). The flexural strength average of the pervious concrete blocks was 4.2 MPa and the specific gravity average was 2.36, with a coefficient of variation of 0.40%. These specific gravity values are typical of pervious concretes used in pavement applications, which tend to be lighter than standard concrete due to the higher amount of air retained in their structure (Cheng et al., 2019).

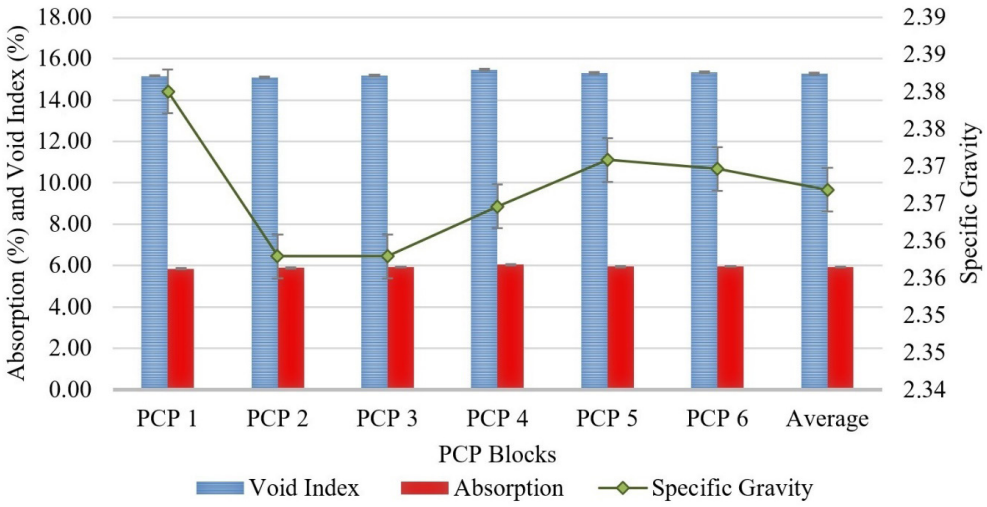

Figure 8. PCP Blocks Characterization according to ASTM C642 (ASTM, 2021c).

3.2. Tomographic analysis of pervious concrete blocks

The tomographic tests (Figure 9) provided additional insights into the internal structure of the pervious concrete, including the average pore diameter, which was determined to be 1.43 mm. This directly influences the material's hydraulic and thermal performance (Merten et al., 2022; Tan et al., 2021; Wang et al., 2022).

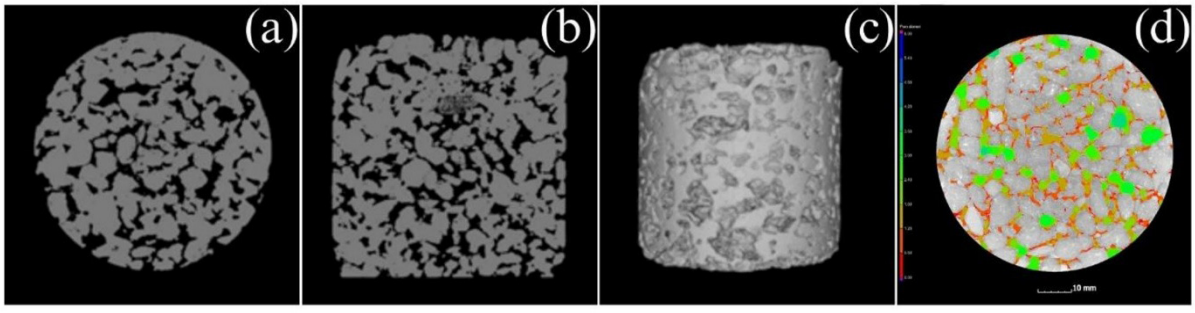

Figure 9. Tomography of the PCP specimen: (a) axial cut; (b) coronal cut; (c) volumetric reconstruction; (d) pore diameter in the axial section.

The computed tomography analysis of the samples, shown in Figure 10, revealed distinct patterns in the porosity distribution between the unclogged and clogged blocks, allowing for the distinction between effective pores (interconnected, allowing fluid flow), isolated pores (not connected to other pores), and total pores (sum of both). The clogging significantly affected the

upper layer of the clogged sample, reducing its porosity by 50% compared to the unclogged specimen. This behavior is consistent with studies indicating that void clogging predominantly occurs at the surface, resulting in 9% lower porosity compared to the lower half of the pervious concrete specimen (Wang et al., 2022). Clogging reduces permeability by hindering water flow and increasing flow resistance within the porous structure, making the material less effective for urban drainage applications (Razzaghmanesh and Beecham, 2018).

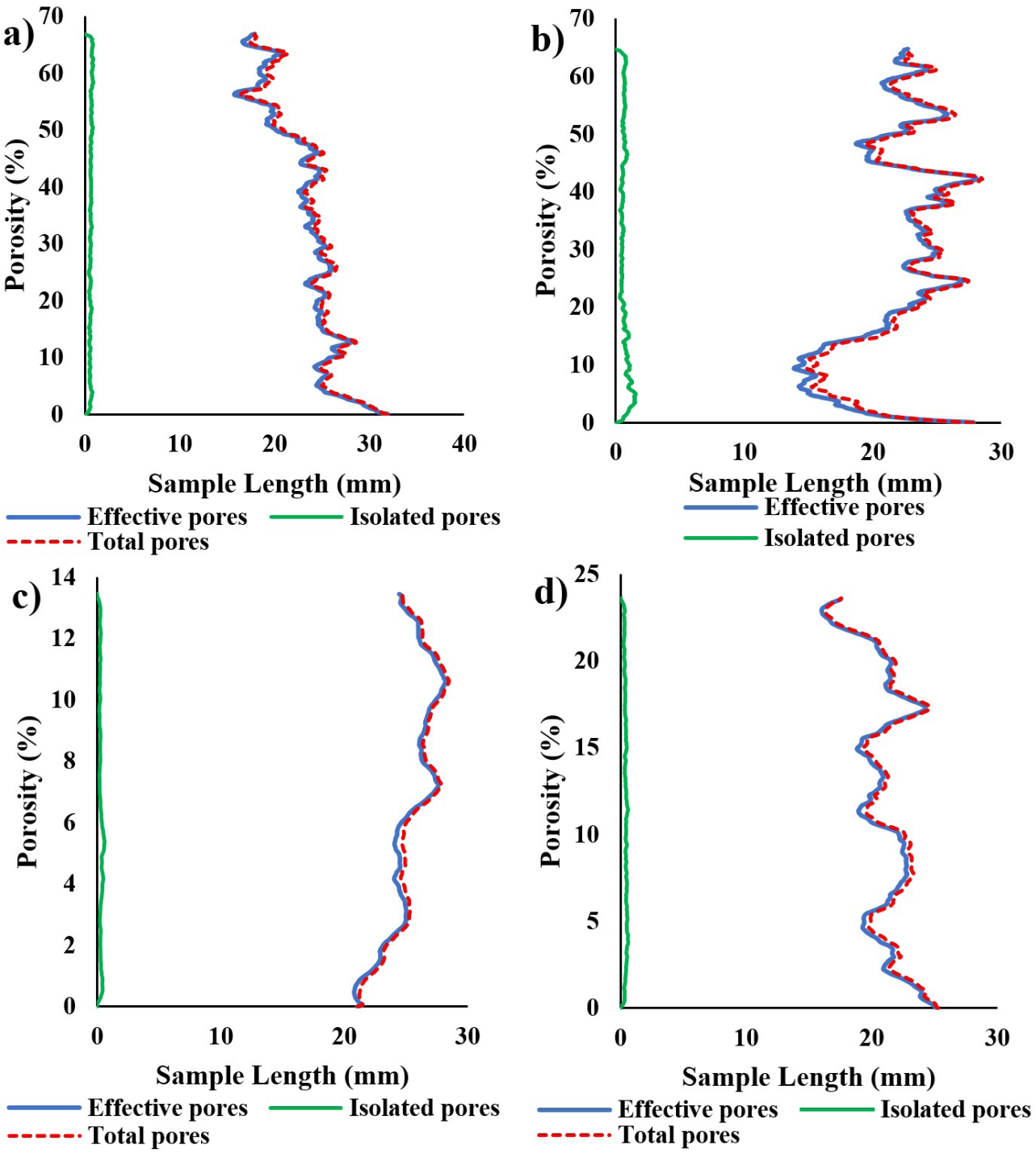

Figure 10. Porosity distribution along the sample length for PCP test specimen: (a) Clean PCP 1; (b) Clean PCP 2; (c) Upper part of the clogged specimen; (d) Lower part of the clogged specimen.

3.3. Permeability results

PCP blocks permeability was evaluated according to ASTM C1701/C1701M (ASTM, 2023). After 20 clogging cycles, the average reduction in permeability was 97%, as shown in Figure 11, like the reduction reported by Tong (2011), who also observed a significant drop. Permeability loss is one of the main challenges of PCP, directly impacting its ability to manage stormwater runoff.

The drastic reduction in permeability can be attributed to the clogging of pores by fine sand particles, which form a compact layer that hinders water infiltration. This finding is corroborated by the tomographic analysis (Figure 10), which revealed a porosity reduction of up to 50% in the upper layer of the clogged blocks. The decrease in permeability is also a direct result of the average pore size of the pervious concrete, which was determined to be 1.43 mm through tomographic tests, and the granulometric distribution of the clogging material. For instance, 22% of the clogging material consists of particles smaller than 6 mm, which are more prone to clogging the pores.

Comparing the results with the literature, only the blocks in their initial state (clean) met the minimum permeability criterion of 10^{-3} m/s recommended by the standard. The 97% loss in permeability after 20 cycles, which simulate approximately 20 years of use, highlights the necessity of periodic maintenance to ensure the pavement's functionality over time (Cheng et al., 2019; Merten et al., 2022). Clogging is therefore not just a theoretical problem but a practical limitation that must be considered in the design and management of PCP.

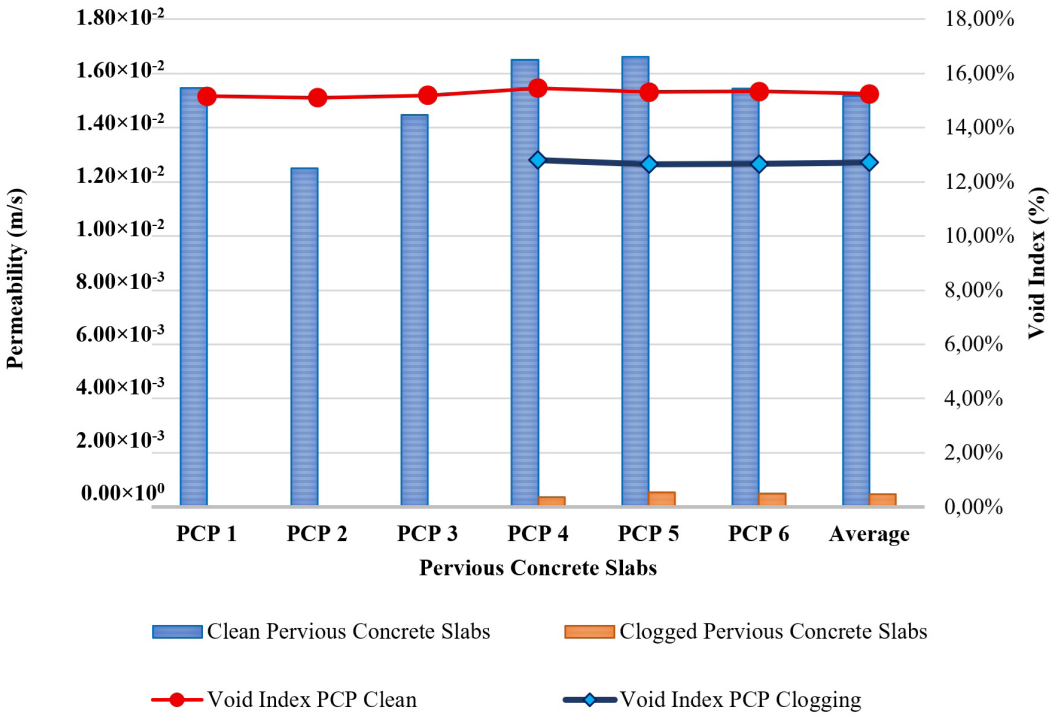

Figure 11. Permeability coefficient of clean and PCP blocks and clogged PCP blocks.

3.4. Surface temperature analysis of pervious concrete blocks

Surface temperature test of PCP, in clean and clogged states, was conducted under full solar exposure from 5:00 a.m. to 7:00 p.m., recording surface temperature (T_{sup}), air temperature (T_{ar}) and relative humidity (%RH) every 30 minutes.

As shown in Figure 12, clean blocks exhibited surface temperatures on average 1.25 °C higher than those observed for clogged ones, during the period of solar exposure. This indicates a higher heat absorption capacity of unclogged surfaces.

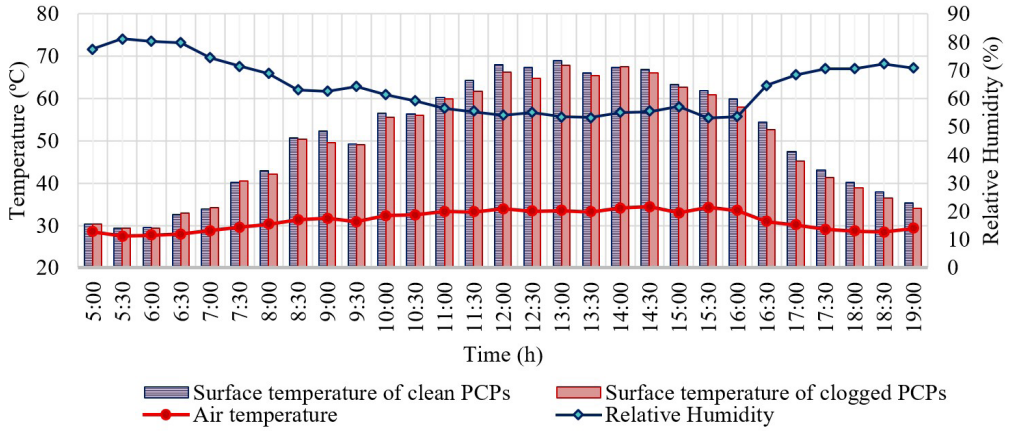

Figure 12. Surface temperature of PCP blocks in clean and clogged states.

Surface temperature of clean blocks was 1.25 °C higher on average than that of clogged blocks due to the voids presented on the surface of the clean blocks. The irregular and porous surface texture contributes to increased heat absorption, as observed by Seifeddine, Amziane and Toussaint (2023) and Tan et al. (2021). This pattern is evidenced in Figure 13, which displays thermal images of the blocks. In these images, clean blocks exhibit colors indicative of higher temperatures compared to clogged ones. Indeed, dense concrete without pores tends to exhibit lower T_{sup} than pervious concrete under similar solar exposure conditions (Peixoto et al., 2023; Tan et al., 2021).

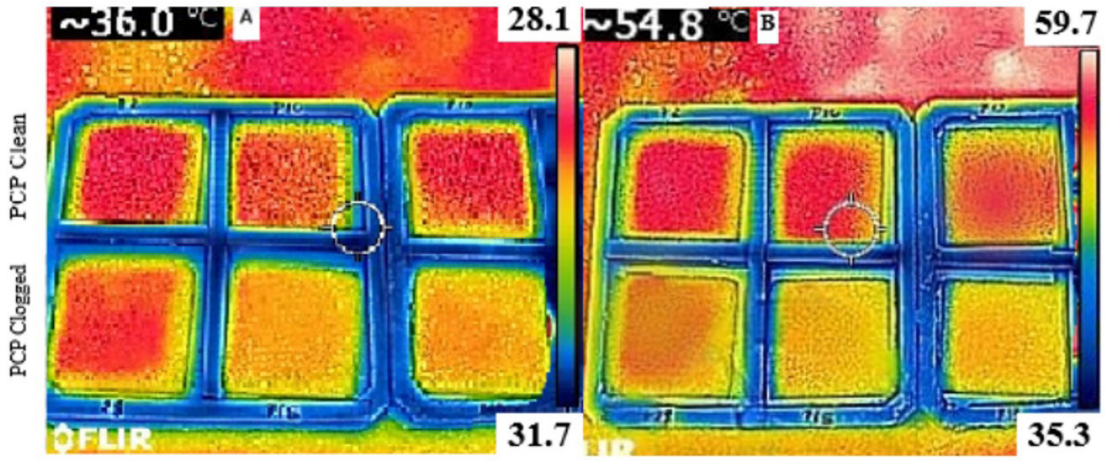

Figure 13. Thermal images of PCP in a clean (top blocks) and clogged (bottom blocks) stages during the day: (a) 9:30 a.m.; (b) 11:30 a.m.

During the cooling phase, the clogged blocks demonstrated 12% higher efficiency compared to the clean PCP blocks in the period between 1:30 p.m. and 5:00 p.m. Moreover, as shown in Figure 14, the reflectance of pervious concrete decreases over time as porosity increases, which is

in line with findings from Zhang, Jiang and Liang (2015) and Lu et al. (2023). The clogged blocks, with reduced porosity due to sediment accumulation, exhibited an average reflectance 7% higher than the clean blocks in the period from 5:30 AM to 7:00 PM. This reduction in reflectance of the clean PCP blocks is attributed to the absorptive nature of the cavities present in pervious concrete, which increases light scattering and absorption, consequently reducing its ability to reflect solar radiation (Lu et al., 2023; Zhang, Jiang and Liang, 2015).

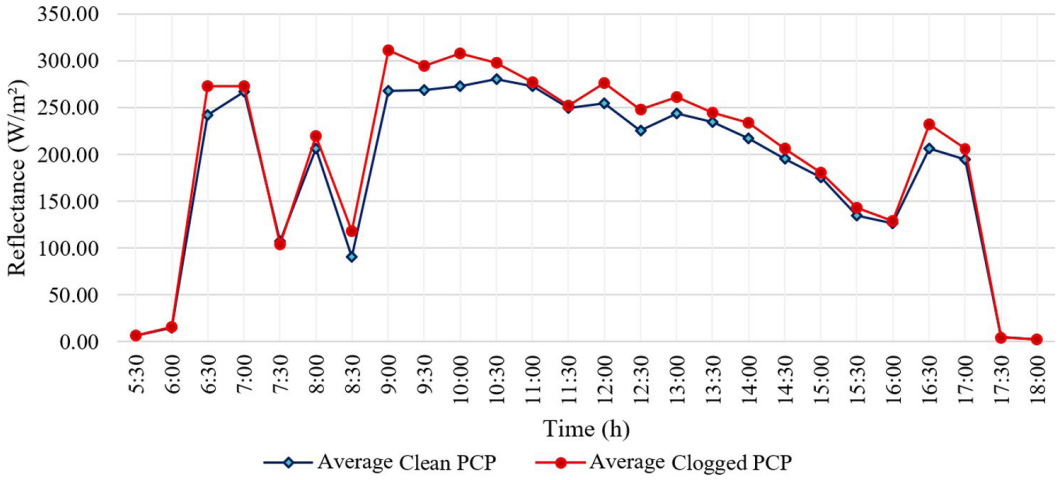

Figure 14. Effect of porosity and clogging on the reflectance of pervious concrete.

The direct influence of average air temperature and relative humidity on reflectance variation over time, as illustrated in Figure 14, reinforces the sensitivity of pervious concrete to environmental conditions. This thermal behavior is in accordance with the findings of Chen et al. (2019a) and Qin and Hiller (2016), highlighting the need to consider both material characteristics and climatic conditions, when designing permeable pavements.

The dry and rough surface when blocks are clean have lower reflectance, absorbing more thermal energy (Seifeddine, Amziane and Toussaint, 2023). With clogging, the pores are partially filled, smoothing the surface and resulting in lower surface temperatures. For cleaning pervious concrete to significantly reduce surface temperature reduction, water must be in its pores, allowing cooling by evaporation (Qin and Hiller, 2016).

The influence of air temperature and relative humidity on the surface temperature of pervious concrete blocks, both in clean and clogging states, was evaluated using generalized least squares (GLS) regression models, adjusting for temporal autocorrelation in the data. The prediction equation obtained for the clean blocks was described below (Equation 8).

$$T_{clean} = 41.766 + 2.068 \times T_{air} - 0.865 \times Relative\ Humidity \left(R^2 = 0.947\right) \quad (8)$$

The coefficient associated with air temperature (2.068; p=0.0331) indicates that a 1.00°C increase in air temperature corresponds to an average increase of 2.07°C in the surface temperature of the clean blocks. On the other hand, the coefficient for relative humidity (-0.865; p=0.0007) shows that a 1% increase in humidity results in a 0.87°C decrease in the slab temperature. For the clogged blocks, the prediction equation is described below (Equation 9).

$$T_{clogging} = -6.548 + 3.038 \times T_{air} - 0.598 \times Relative\ Humidity \left(R^2 = 0.946\right) \quad (9)$$

In this case, air temperature presented a higher coefficient $(3.038; p = 0.0020)$, indicating that each 1.00°C increase in air temperature results in a 3.04°C increase in the temperature of the clogged blocks. The effect of relative humidity was smaller $(-0.598; p = 0.0147)$, implying a 0.60°C reduction in the temperature of the blocks for each 1% increase in humidity. The results show that air temperature has a greater impact on the clogged blocks, while relative humidity affects the clean blocks more intensely. The results show an R^2 of 0.947 for both the clean and clogged blocks, indicating that the model explains 94.7% of the variation in surface temperature, it is in Figure 15.

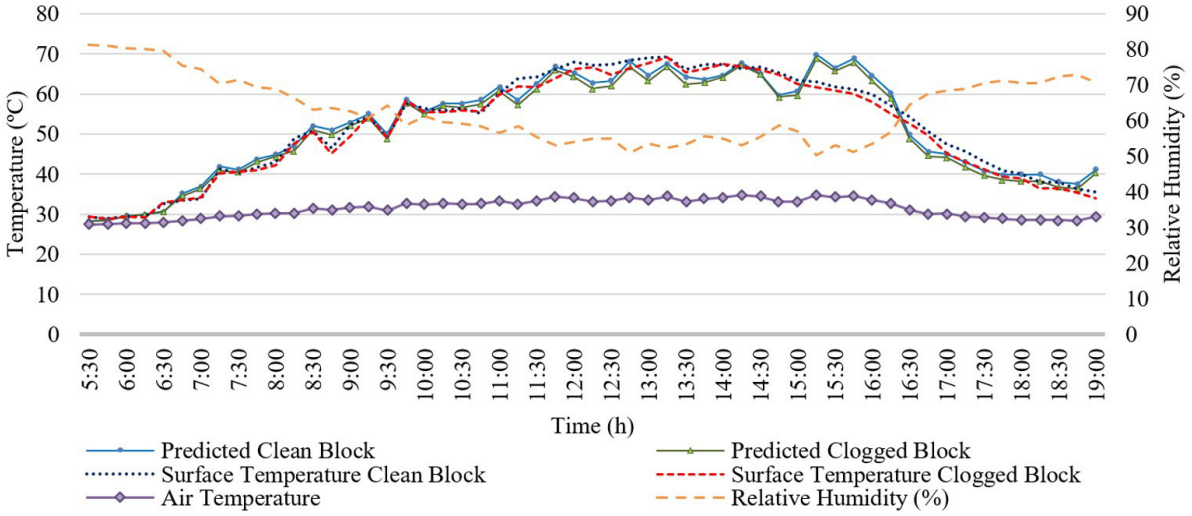

Figure 15. Surface temperature of clean and clogged blocks with air temperature and relative humidity.

3.5. Analysis of the thermal conductivity of pervious concrete blocks

The determination of the thermal conductivity of the pervious concrete blocks was conducted using algebraic calculations, considering the proportions of the components of the pervious concrete in the clean state, as well as the respective thermal conductivities of each component. For the clogged blocks, the volumetric proportion of sand that filled the voids of the pervious concrete was analyzed. For this, the bulk density of the clogging sand was obtained, which presented a value of 1,466.73 kg/m^3.

The analysis of the specific gravity of the sand allowed for determining the percentage of clogging sand present in the pores of the PCP blocks, in addition to quantifying the reduction in the void index, evidencing the filling of the pores by the material, as shown in Table 3.

Table 3: Proportions of Materials Used in the Calculation of Thermal Conductivity Predicted for Pervious Concrete

Proportions	Clean PCP	Clogged PCP
Void Index	0.153	0.121
Coarse Aggregate	0.546	0.546
Fine Aggregate	0.162	0.162
Paste	0.139	0.139
Clogging Sand	0	0.032

Following the methodology described by Nassiri and Nantasai (2017), the thermal conductivity values for PCP in both clean and clogged states were determined. Results indicated a 0.41% increase in thermal conductivity due to clogging, with clean PCP blocks exhibiting an average thermal conductivity of 0.779 W/m.K, while clogged blocks reached 0.782 W/m.K. This variation highlights the impact of clogging on the material's heat conduction capacity. The increase in thermal conductivity in clogged blocks is attributed to the partial replacement of air voids by sand particles, as sand possesses a thermal conductivity coefficient 85.7% higher than air, facilitating faster heat exchange with the environment. Despite this increase, clogged blocks exhibited lower surface temperatures. This occurs because clogging reduces the exposed pore area, resulting in less surface contact with the environment. As Zhang, Jiang and Liang (2015) point out, surfaces with higher porosity tend to absorb more heat due to increased roughness. Thus, the smoother surface of the clogged PCP decreases solar radiation absorption, reducing heat gain during the day.

According to Chen et al. (2019a), the thermal conductivity coefficients of pervious concrete range from 0.47 W/m.K to 0.82 W/m.K. The values obtained for the PCP blocks in this study for both, the clean state (0.779 W/m.K) and the clogged state (0.782 W/m.K), indicating that results fall within the range reported in the literature. To assess the difference between these states, a one-way analysis of variance (ANOVA) was performed, testing the null hypothesis that there is no significant difference between the groups.

The average thermal conductivity was 0.7800 W/m.K for the three clean blocks and 0.7824 W/m.k for the three clogged ones, with variances of 3.47×10^{-11} and 2.53×10^{-7}, respectively. The obtained F-value was 65.87, exceeding the critical value of 7.71, and the p-value was 0.0013, indicating a statistically significant difference and rejecting the null hypothesis. These results confirm clogging influences the thermal conductivity of pervious concrete.

4. CONCLUSIONS

This study investigated the hydraulic and thermal behavior of pervious concrete pavement (PCP) under clogging conditions, using laboratory tests and tomographic analyses to evaluate the impact of clogging on the material's properties. The permeability of the PCP slabs was severely reduced by 97.13% after the clogging process, highlighting that clogging is a significant limitation and underscoring the critical need for periodic maintenance to preserve the pavement's hydraulic efficiency over time.

Clogging also led to a statistically significant increase of 0.41% in the thermal conductivity of the blocks, which rose from an average of 0.779 W/m·K to 0.782 W/m·K. This change is attributed to the replacement of air, a thermal insulator, within the pores with sand particles. The thermal behavior of PCP differed between clean and clogged conditions, with clean blocks showing surface temperatures that were, on average, 1.25 °C higher than clogged blocks under solar exposure. This difference is due to the porous, irregular surface of clean concrete, which promotes greater solar radiation absorption, while the smoother, clogged surface absorbs less heat.

The tomographic analysis further revealed that clogging primarily affects the upper layer of the specimens, reducing its porosity by 50% compared to the unclogged specimens. In summary, while pervious concrete demonstrates good initial performance, clogging is a critical limitation that negatively impacts permeability, although it has a marginal effect on thermal performance. These findings have significant practical implications: when managing low-impact development structures, the balance between hydraulic and thermal behaviors must be carefully evaluated to promote effective "sponge cities".

This study investigated the hydraulic and thermal behavior of PCP, focusing on the influence of clogging on permeability, thermal conductivity and cooling efficiency. Through laboratory tests and tomographic analyses, it was possible to evaluate the impact of different clogging states on the material's properties.

The initial characterization of the PCP showed a void index of 15.26%, a value that ensures good infiltration capacity and effective surface runoff control. However, permeability was severely reduced (97.13%) after the clogging process, highlighting the need for periodic maintenance to preserve hydraulic efficiency over time.

The analysis of thermal conductivity reinforced the influence of clogging on the material's thermal properties, with a 0.41% increase in the conductivity of clogged blocks. This is attributed to the replacement of air with sand in the pores, which increases the heat conduction capacity. The difference in thermal conductivity between clean and clogged states highlights that clogging not only impacts permeability but also alters the thermal behavior of pervious concrete.

The thermal behavior of PCP differed between clean and clogged conditions. While air is a better thermal insulator, the irregular, porous surface of clean pervious concrete promotes greater solar radiation absorption due to increased surface area and exposed voids, reducing reflectance and enhancing heat retention. However, the difference in heat absorption between clean and clogged blocks was only 1.73%, indicating a marginal thermal impact. Clogged PCP, with partially obstructed pores, showed slightly lower heat uptake and more efficient cooling. This suggests that surface clogging may have a minor but beneficial role in reducing pavement temperatures under intense solar radiation, potentially contributing to UHI mitigation. Future studies are recommended to address the limitation of the block's insulation from the substrate by testing under realistic boundary conditions, considering the thermal interaction with underlying pavement layers and the subgrade.

The tomographic analysis identified the clogging affected the upper layer of the clogged sample, reducing its porosity by 50% compared to the unclogged specimen, where void clogging predominantly occurs at the surface. This emphasizes the importance of periodic maintenance to optimize the performance of pervious concrete. In summary, while pervious concrete demonstrates good initial performance, clogging is a critical limitation that negatively impacts permeability, although it has a marginal effect on thermal performance. These findings have significant practical implications: when managing low-impact development structures, the balance between hydraulic and thermal behaviors must be carefully evaluated to promote effective "sponge cities".

AUTHORS' CONTRIBUTIONS

KL: Writing – Original Draft, Conceptualization, Methodology, Validation, Investigation, Formal analysis, Data Curation; LVSR: Methodology, Validation, Investigation, Data Curation; ACDA: Methodology, Validation; AEBC: Resources, Writing – Review and Editing, Supervision; VTFCB Conceptualization, Resources, Writing - Review and Editing, Supervision, Project administration, Funding acquisition.

CONFLICTS OF INTEREST STATEMENT

The authors declare that there is no conflict of interest.

USE OF ARTIFICIAL INTELLIGENCE-ASSISTED TECHNOLOGY

The authors declare that no artificial intelligence tools were used in the research reported here or in the preparation of this article.

DATA AVAILABILITY STATEMENT

The data generated and analyzed during this study are included in this published article, as evidenced by the presented figures, adjusted models, and analyses.

REFERENCES

ASTM (2021a) *D6913/D6913M-17: Standard Test Methods for Particle-Size Distribution (Gradation) of Soils Using Sieve Analysis.* West Conshohocken, PA: ASTM International.

ASTM (2021b) *D7263-21: Standard Test Methods for Laboratory Determination of Density (Unit Weight) of Soil Specimen*. West Conshohocken, PA: ASTM International.

ASTM (2021c) *C642-21: Standard Test Method for Density, Absorption, and Voids in Hardened Concrete.* West Conshohocken, PA: ASTM International.

ASTM (2022) *C78/C78M-22: Standard Test Method for Flexural Strength of Concrete (Using Simple Beam with Third Point Loading)*. West Conshohocken, PA: ASTM International.

ASTM (2023) *C1701/C1701M-17a: Standard Test Method for Infiltration Rate of In Place Pervious Concrete*. West Conshohocken, PA: ASTM International.

Bin Yahaya, N. (2010) *An Exploration of Co-Development Within the Malaysian Automotive Industry*. Doctor thesis. Cranfield University. Bedford, UK.

Bonicelli, A. and L.R. Pianeta (2019) Performance and applications of pervious concrete pavement material as an overlay on existent concrete slabs. *IOP Conference Series. Materials Science and Engineering*, v. *471*, p. 032061. DOI: 10.1088/1757-899X/471/3/032061.

Chen, J.; R. Chu; H. Wang *et al*. (2019a) Alleviating urban heat island effect using high-conductivity permeable concrete pavement. *Journal of Cleaner Production*, v. *237*, p. 117722. DOI: 10.1016/j.jclepro.2019.117722.

Chen, J.; H. Wang; P. Xie et al. (2019b) Analysis of thermal conductivity of porous concrete using laboratory measurements and microstructure models, *Construction & Building Materials*, v. *218*, p. 90-8. DOI: 10.1016/j.conbuildmat.2019.05.120.

Cheng, Y.-Y.; S.-L. Lo; C.-C. Ho *et al*. (2019) Field testing of porous pavement performance on runoff and temperature control in Taipei City. *Water*, v. *11*, n. 12, p. 2635. DOI: 10.3390/w11122635.

Ding, Z.; P. Li; X. Wu *et al*. (2020) Evaluation of the contact characteristics of graded aggregate using coarse aggregate composite geometric indexes. *Construction & Building Materials*, v. *247*, p. 118608. DOI: 10.1016/j.conbuildmat.2020.118608.

DNIT (2020) *432-ME: Agregados: Determinação das Propriedades de Forma por Meio do Processamento Digital de Imagens (PDI)-Método de Ensaio.* Brasília: DNIT.

El-Hassan, H.; P. Kianmehr and S. Zouaoui (2019) Properties of pervious concrete incorporating recycled concrete aggregates and slag. *Construction & Building Materials*, v. *212*, p. 164-175. DOI: 10.1016/j.conbuildmat.2019.03.325.

Guan, X.; J. Wang and F. Xiao (2021) Sponge city strategy and application of pavement materials in sponge city. *Journal of Cleaner Production*, v. *303*, p. 127022. DOI: 10.1016/j.jclepro.2021.127022.

Hendel, M.; S. Parison; A. Grados *et al*. (2018) Which pavement structures are best suited to limiting the UHI effect? A laboratory-scale study of Parisian pavement structures. *Building and Environment*, v. *144*, p. 216-229. DOI: 10.1016/j.buildenv.2018.08.027.

Isaia, G.C. (2007) *Materiais de Construção Civil e Princípios de Ciências e Engenharia de Materiais.* São Paulo: IBRACON.

Kia, A.; H.S. Wong and C.R. Cheeseman (2017) Clogging in permeable concrete: a review. *Journal of Environmental Management*, v. *193*, p. 221-233. DOI: 10.1016/j.jenvman.2017.02.018. PMid:28222353.

Kovác, M. and A. Sicáková (2017) Pervious concrete as a sustainable solution for pavements in urban areas. *In Proceedings of 10th International Conference "Environmental Engineering"*. Lithuania: Vilnius Tech. DOI: 10.3846/enviro.2017.031.

Lu, Y.; Y. Qin; C. Huang *et al*. (2023) Albedo of pervious concrete and its implications for mitigating urban heat island. *Sustainability*, v. *15*, n. 10, p. 8222. DOI: 10.3390/su15108222.

Maroof, M.A.; A. Mahboubi and A. Noorzad (2020) A new method to determine specific surface area and shape coefficient of a cohesionless granular medium. *Advanced Powder Technology*, v. *31*, n. 7, p. 3038-3049. DOI: 10.1016/j.apt.2020.05.028.

Mata, L. A. (2008). *Sedimentation of Pervious Concrete Pavement Systems*. Dissertation. NC State University. Raleigh, NC.

Merten, F.R.M.; V.F.P. Dutra; H.L. Strieder *et al*. (2022) Clogging and maintenance evaluation of pervious concrete pavements with recycled concrete aggregate. *Construction & Building Materials*, v. *342*, p. 127939. DOI: 10.1016/j.conbuildmat.2022.127939.

Miao, Y.; X. Liu; Y. Hou *et al*. (2019) Packing characteristics of aggregate with consideration of particle size and morphology. *Applied Sciences*, v. *9*, n. 5, p. 869. DOI: 10.3390/app9050869.

Mindess, S. (2019). Resistance of concrete to destructive agencies. In Hewlett, P.C. (ed.) *Lea's Chemistry of Cement and Concrete*. Oxford: Butterworth-Heinemann, p. 251-283.

Moretti, L.; P. Di Mascio and C. Fusco (2019) Porous concrete for pedestrian pavements. *Water*, v. *11*, n. 10, p. 2105. DOI: 10.3390/w11102105.

Nassiri, S. and B. Nantasai (2017) Thermal conductivity of pervious concrete for various porosities. *ACI Materials Journal*, v. *114*, n. 2, p. 265-271. DOI: 10.14359/51689492.

Neville, A.M. (1995) *Properties of Concrete* (Vol. *4*). London: Longman.

Peixoto, N.G.M.; L.V.S. Ribas; L.M. Monteiro *et al*. (2023) Avaliação do comportamento térmico de materiais empregados em projeto de requalificação viária na cidade de Fortaleza. *In Anais do 17º Encontro Nacional de Conforto no Ambiente Construído*. Porto Alegre: ANTAC, p. 1-10. DOI: 10.46421/encac.v17i1.4001.

Qin, Y. and J.E. Hiller (2016) Water availability near the surface dominates the evaporation of pervious concrete. *Construction & Building Materials*, v. *111*, p. 77-84. DOI: 10.1016/j.conbuildmat.2016.02.063.

Razzaghmanesh, M. and S. Beecham (2018) A review of permeable pavement clogging investigations and recommended maintenance regimes. *Water*, v. *10*, n. 3, p. 337. DOI: 10.3390/w10030337.

Rossetto, R.; A. Lenti; L. Ercoli *et al*. (2023) Infiltration performance evaluation of a 15-year-old concrete grid paver parking area (Italy). *Blue-Green Systems*, v. *5*, n. 2, p. 294-305. DOI: 10.2166/bgs.2023.043.

Seifeddine, K.; S. Amziane and E. Toussaint (2022) Thermal behavior of pervious concrete in dry conditions. *Construction & Building Materials*, v. *345*, p. 128300. DOI: 10.1016/j.conbuildmat.2022.128300.

Seifeddine, K.; S. Amziane and E. Toussaint (2023) State of the art on the hydraulic properties of pervious concrete. *Road Materials and Pavement Design*, v. *24*, n. 11, p. 2561-2596. DOI: 10.1080/14680629.2022.2164332.

Spoorthy, B.M. and A.K. Chandrappa (2023) Design methodology and clogging investigation of 2-layered pervious concrete (2L-PC) for pavement applications. *The International Journal of Pavement Engineering*, v. *24*, n. 2, p. 2111566. DOI: 10.1080/10298436.2022.2111566.

Tahmasebi, P. (2018) Packing of discrete and irregular particles. *Computers and Geotechnics*, v. *100*, p. 52-61. DOI: 10.1016/j.compgeo.2018.03.011.

Taleghani, M. (2018) Outdoor thermal comfort by different heat mitigation strategies: a review. *Renewable & Sustainable Energy Reviews*, v. *81*, p. 2011-2018. DOI: 10.1016/j.rser.2017.06.010.

Tan, K.; Y. Qin; T. Du *et al*. (2021) Biochar from waste biomass as hygroscopic filler for pervious concrete to improve evaporative cooling performance. *Construction & Building Materials*, v. *287*, p. 123078. DOI: 10.1016/j.conbuildmat.2021.123078.

Tong, B. (2011) *Clogging Effects of Portland Cement Pervious Concrete*. Doctor thesis. Iowa State University. Ames, IA.

Wang, J.; Q. Meng; K. Tan *et al*. (2018) Experimental investigation on the influence of evaporative cooling of permeable pavements on outdoor thermal environment. *Building and Environment*, v. *140*, p. 184-193. DOI: 10.1016/j.buildenv.2018.05.033.

Wang, X.; Y. Wang; X. Ge *et al*. (2022) The quantitative assessment of clogging and cleaning effects on the permeability of pervious concrete. *Construction & Building Materials*, v. *335*, p. 127455. DOI: 10.1016/j.conbuildmat.2022.127455.

Xie, N.; M. Akin and X. Shi (2019) Permeable concrete pavements: a review of environmental benefits and durability. *Journal of Cleaner Production*, v. *210*, p. 1605-1621. DOI: 10.1016/j.jclepro.2018.11.134.

Xiong, B.; H. Gao; X. Lu *et al*. (2023) Influence of maximum paste coating thickness without void clogging on the pore characteristics and seepage flow of pervious concrete. *Construction & Building Materials*, v. *392*, p. 131979. DOI: 10.1016/j.conbuildmat.2023.131979.

Xiong, Q.; T.G. Baychev and A.P. Jivkov (2016) Review of pore network modelling of porous media: Experimental characterisations, network constructions and applications to reactive transport. *Journal of Contaminant Hydrology*, v. *192*, p. 101-117. DOI: 10.1016/j.jconhyd.2016.07.002. PMid:27442725.

Yang, H.; K. Yang; Y. Miao *et al*. (2020) Comparison of potential contribution of typical pavement materials to heat island effect. *Sustainability*, v. *12*, n. 11, p. 4752. DOI: 10.3390/su12114752.

Yuan, J.; X. Chen; S. Liu *et al*. (2018) Effect of water head, gradation of clogging agent, and horizontal flow velocity on the clogging characteristics of pervious concrete. *Journal of Materials in Civil Engineering*, v. *30*, n. 9, p. 04018215. DOI: 10.1061/(ASCE) MT.1943-5533.0002410.

Zhang, R.; G. Jiang and J. Liang (2015) The albedo of pervious cement concrete linearly decreases with porosity. *Advances in Materials Science and Engineering*, v. *2015*, p. 1-5. DOI: 10.1155/2015/746592.

Zimmerman, R.W. (1989) Thermal conductivity of fluid-saturated rocks. *Journal of Petroleum Science Engineering*, v. *3*, n. 3, p. 219-227. DOI: 10.1016/0920-4105(89)90019-3.